Application of FEA Metal Cutting Model for Determining Surface Roughness

A. E. Rodygina

Irkutsk State Technical University,
664074 Russia, Irkutsk, Lermontova street, 83.
rodygina.ae@gmail.com

***Abstract* – In conditions of the rigid technological system and an unworn tool the strain constituent of microirregularity height has the largest value. The present work suggests a research method for forming strain constituents of roughness when cutting surfaces with the use of FEM. Based on the described model the basic regularities of the strain component formation depending on some machining parameters are identified.**

Keyword – Constrained cutting, FEA, Surface roughness, Strain component, Geometrical component

I. INTRODUCTION

Metal cutting is an exclusively complicated process inclusive of plastic flow of a metal being cut, under strains, which cannot be reached during the other processes, and its failure in marginal conditions. On contact surfaces of a tool and material being worked friction is generated, close to dry by its nature. Contact temperatures for hard alloys and non-metallic tool materials can exceed 1000°C. On the strength of reasons shown, the basic method for studying surface roughness, along with the other phenomena accompanying the cutting process, became an experimental method implemented in the form of empirical dependences and reference materials.

Along with it, just as like in any other experimentally obtained dependences, fragmentarity is inherent in the results of study of surface roughness, as well as the necessity for their replenishment. The situation is solved by obtaining the analytical dependences. Taking into account the fact that formation of microirregularities on the surface worked is a result of motion of the shaping and processes connected with chip separation, an analytical decision is to be based upon determination of the stress-strain state of a chip formation area, which leads to the formation of residual ridges on the surface worked. Under such a formulation of the task its solution with the use of a system of classical theory of plasticity is linked with big problems inasmuch as the volumetric plastic straining with large degrees takes place. As a consequence, the necessity arises for some serious assumptions which decrease authenticity of the results received.

Development of methods for mathematical modelling opens new opportunities to study the stress-strain state in a cutting area. As the basic criteria for choosing the finite element software to create the planned models, the following ones were accepted

- approach for the cutting process is to be thermomechanical;
- as a result of computations in solid models, large final stresses and strains can be obtained;
- automatic improvement of the distorted finite element mesh is required
- permitting to adjust a rate of tool displacement, and consequently, a rate of strain;
- setting conditions for the contact interaction between a workpiece and a tool.

At the present time the application of a finite element analysis to the study of processes, including the cutting process, is widespread. In most cases the authors' models ([2], [4], [9], [13], [18]) realize the free cutting process, and in particular, the orthogonal cutting. They cannot be used for studying the surface roughness formation process, but they entirely fit in the study of chip deforming processes, the stressed state of a part machined and a layer being cut, and thermal processes as well. Some researchers confine themselves to an initially certain and formed root of chip, i.e there is no material cutting process in dynamics ([9]). The process of chip separation from a workpiece can be implemented by a few ways: either setting nodes, through which the splitting is done ([17]), or designating FE which will "be crumbling" when certain program parameters ([1], [10]) are exceeded; in most cases a function of the rebuilding is used of the distorted finite element mesh ([2], [4], [8], [13], [18]). With respect to the microirregularity formation process, the first two variants do not fit in, inasmuch as it is rather problematic to set similar nodes and FE on two cutting planes. Moreover, the location of the strain component of roughness height parameter loses its significance.

According to the results of the acceptable modelling methods, a system of the non-linear finite element analysis MSC.Marc (MSC.Software Corporation) was chosen.

The main advantages of MSC.Marc are the use of procedure for automatic rebuilding of the finite element model mesh, as it becomes deformed and distorted - the intermediate results are carried over to the renewed mesh, - as well as the capability for modelling absolutely rigid contacting surfaces (discrete or set analytically), which makes it possible to use it for establishing a model of the constrained cutting.

II. Building the Constrained Cutting Model

The main task of modelling was to find the strain component of microirregularities, which makes the greatest contribution to their formation along with the calculated one. When building a geometrical model as the initial one, a scheme of the constrained cutting was accepted, which is realized in linear turning (Fig. 1).

In view of the fact that an analysis of the cutting process requires a short length for the cutting tool pass, and it makes no sense to generate a full model of a workpiece and a cutting tool. When diameters of workpieces are rather large, the element of a part surface in the direction of vector of cutting speed can be regarded as conventionally rectilinear.

Transition from rectilinear motion to circular motion is linked with instability of cutting speed along the length of a cutting edge, and the change of speed is insignificant.

Proceeding on the assumption of these prerequisites, a geometrical model of the constrained cutting was built as a body with mutually orthogonal flat outer boundaries, which also form geometrical residual ridges of the surface machined. The influence of tool was viewed as the introduction of a rigid stamp in half-space. A form and position of the stamp reproduced an area surrounding the point of a straight-turning tool.

As the finite elements for a model, was used Tet4, type 157, representing tetrahedrons of the first order with calculated nodes on the points. A criterion for its selection was that the given type of finite elements is possible for the use under large strains and angular displacements when including the plasticity procedure Large strain–radial return–multiplicative decomposition. Besides, only elements of the first order are supported by calculation subprogram afmesh3d, which provides a function of the remeshing (Adaptive Meshing) when a certain criterion set by the software is exceeded.

With a view to saving resources of computer memory - when calculating a three-dimensional model, an exclusively great number of elements and nodes are formed, and this correspondingly enlarges the stiffness matrix itself - it is necessary to find optimal sizes of FE mesh.

The denser mesh gives a better convergence of results, but along with this, the computing resources consumed and calculated time increase. To find an optimal variant of the mesh, a series of models with parameters was calculated: 0.7; 0.8; 0.9; 1.0; 1.1 and 1.2 sizes of the finite elements from those previously selected as basic elements (edge length average – 0.03 mm, minimum length of edge – 0.008 mm, curvature parameter – 26).

A model with 1.0 coefficient was completely calculated, and it was found that the dependence of calculated time on the percentage of performance can be approximated to a linear form, in case of good convergence in the stiffness matrix. Therefore, to reduce the time of analysis being performed, the calculation was done up to 20 increments. Percentage of performance, time and result were calculated - supposed time of full calculation (Fig. 2, a). It is clear that an optimal variant as per time of performance is 0.9…1.0 area, where an increase in the mesh density does not yet result in the quick growth of the calculated time, but the large coarsening of mesh does not give a significant advantage of time. To evaluate quality of calculation, corresponding to different density of the mesh, the dependence was also established of error for determining a volume of a triangulated strained body with regard to the initial one, depending on a link length, when rebuilding the mesh many times for 5% from the entire calculation (Fig. 2, b). An inflection point is observed. Consequently, in this point there is an optimal correlation of quality of calculation and FE sizes. The trend line has the power-law dependence of the fourth order; an equation of the line is in the field of figure. Consequently, from standard mathematical operations L_{opt}=0.98 basic parameters of the mesh were selected correctly from the outset.

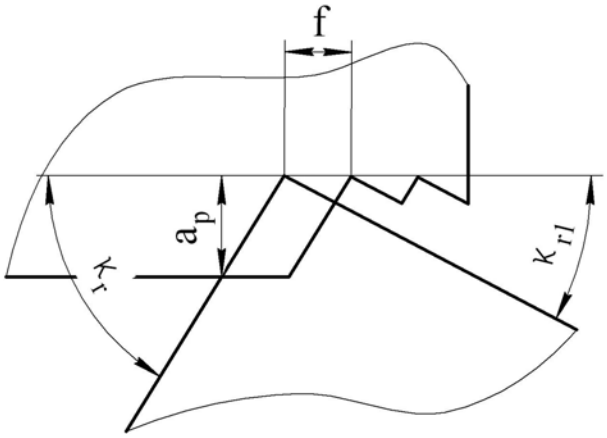

Fig. 1. Scheme of the constrained cutting

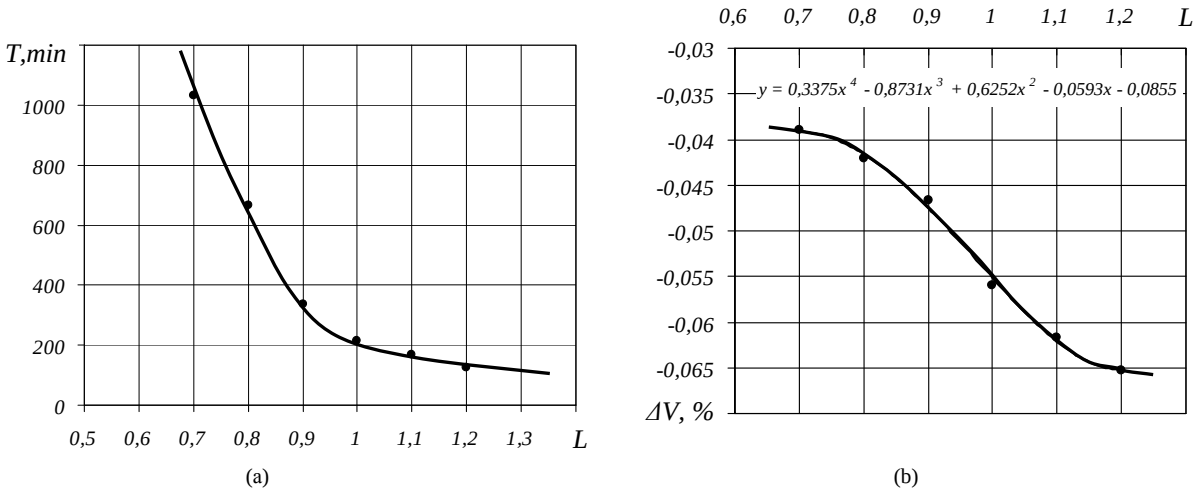

Fig. 2. Dependence of time of full model calculation (a) and error of volume of a strained body for 5% performance of model calculation (b) from the finite element mesh edge length, in units from the gauge length.

The geometrical model with the finite element mesh accepted for the study is shown in Fig. 3.

As boundary conditions (replacement of a rejected part section), rigid planes were accepted, which fix the model and prevent any displacement - basic motion is done by a stamp-cutter. Load is represented by the contact interaction of a strained workpiece body and a rigid heat-conductive cutter body.

When building models, steels were used from the standard MSC.Marc materials, where for each material a complex of mechanical properties was presented, inclusive of properties depending on temperature. The last was of much importance because, according to ([6], [15]), there is no the single or common stress-strain curve for compression-tension and cutting. Therefore, it is hard to set all material properties, especially the plastic ones, without an appropriate experimental basis.

According to the classification of material machining groups, structural C45 и 41Cr4, ISO 683–1, as well as stainless corrosion-resistant steel of austenitic class X10CrNiTi18–9, ISO 4955 were selected. As for properties of the materials machined, some assumptions were made. It was accepted as homogeneous, solid and isotropic, i.e. anisotropy, emerging from the previous pass of a cutting tool, was not taken into account.

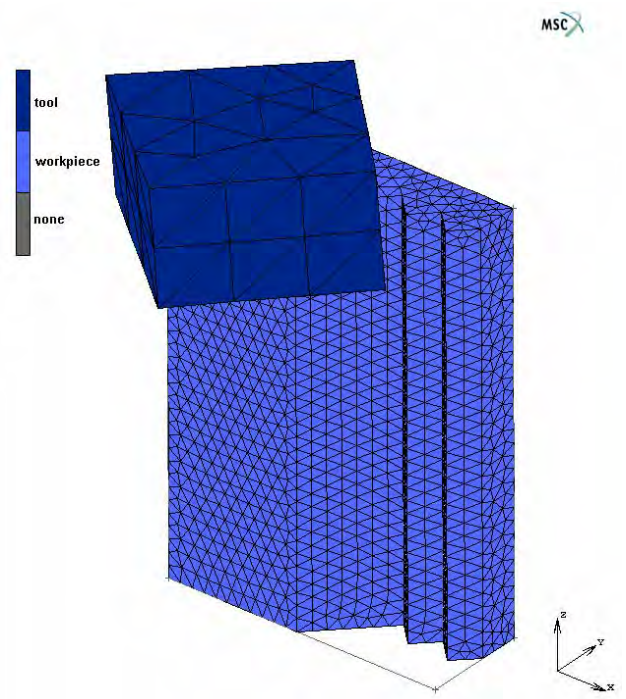

Fig. 3. Geometrical model of the constrained cutting with the finite element mesh

MSC.Marc makes it possible to show material behaviour beyond the flow limits, thus dividing elasticity and plasticity. Elastic properties of the material specify the elasticity modulus E=2.1e+11 Pa and Poisson ratio. Plastic properties are set by piecewise linear flow curves.

In view of the fact that the cutter was considered as an absolutely rigid wedge (as an assumption, strain of the tool itself was not considered as insignificant), only thermal properties were set for it, and namely, heat conductivity factor, specific heat capacity and material density as well Table I.

TABLE I
Properties of Tool Materials

Grade of tool material	**Heat conductivity factor, N/(s*K)**	**Specific heat capacity $mm^2/(s^2*K)$**	**Density ton/mm^3**
hard metal group WC-TiC-Co	27	1.8e+8	1.15e-8
hard metal group WC-Co	57	1.6e+8	1.46e-8
mixed or black ceramics Al_2O_3+TiC	4	8e+8	4.2e-9
CBN	70	5.5e+8	3.45e-9

An assumption was made for the models that the cutting wedge has zero cutting edge radius, otherwise, a number of the finite elements, as a result of the mesh generation, increases unacceptably for system resources of computing machines. As is known, a real cutting blade is not perfectly sharp. It always has a cutting edge radius, a value of which, depending on a tool grinding process and tool material, usually finds itself in the limits 7…15 μm. In the process of wear the radius of the enlarged cutting edge, reaching ρ=20…50 μm for high-speed steel, and ρ=10…20 μm ([11]) for hard alloys. Along with it, on the rounded surface there are always stagnant phenomena, levelling the cutting blade shapes ([3]). Notice was also taken of the fact that the curved part of surface of chip contact with the front surface takes up a negligibly small portion from the total contact area.

When choosing machining conditions, the following were taken as the basic ones:

– cutting tool: rake angle γ=0°; cutting edge inclination angle λ=0°, side relief angle α=8°; end relief angle α_1=5.5°; tool cutting edge angles κ_r=κ_{r1}=45°; tool nose radius r_ε=0,

– process parameters: depth of cut a_p=0.15 mm; feed f=0.1 mm/rev; cutting speed v=175 m/min (2920 mm/s; in SU MSC. Marc).

In the process of modelling the rake angle, the tool cutting edge angle, minor cutting edge angle, feed and cutting speed were altered. The varying was done according to the principle of single-factor experiment. The initial data, for which the finite element models were built and calculated, are shown in Table II.

The tool displacement relative to a workpiece was set with rates shown in Table II. The cutter displacement limitation was set in contact conditions. A value of displacement, equal to 0.7 mm, was taken for 100%. Such a small value was set owing to the fact that at the moment of an increase in the cutter displacement, an abrupt increase is observed in time of calculation and in computing the resources consumed. Along with it, the given value is rather sufficient to form a normal chip root with the start point of curling.

TABLE III
Initial Data for Building the Models

Model number	γ,°	λ,°	κ_{r1},°	f, mm/rev	v, m/min	**Grades of steel**
011	0	0	45	0,1	100	C45, 41Cr4 X10CrNiTi18–9
012					175	
013					250	
021			5		175	
022			15			
023			30			
031	-5		45			
032	5					
033	10					
041	0	-5				
042		5				
051		0		0,05		
052				0,15		
053				0,20		

Setting parameters of the automatic mesh redecomposition and transferring intermediate results to the renewed mesh (Adaptive Meshing) were also taken into account. This is necessary in conditions of large plastic strains in the cutting process. A criterion for the mesh redecomposition was a number of increments –Increment Frequency – every other increment.

Parameters of the rebuilt mesh practically always correspond to the initial values of finite elements. The lesser value of the element edge length gives a more accurate calculation, but along with it, it loads computing resources harder – the more harder the calculation goes further, inasmuch as a chip becomes separated and the total area of strained body grows (the highest density of mesh on the surface; in its depth the mesh becomes coarsened to reduce the resources consumed). In the same manner goes the division of curvilinear surfaces: the higher value, the more accurately curvilinear surfaces are reflected. Therefore, a value a circumference division was provided for in advance, proceeding from the minimum value of FE edge length.

Contact interaction of a workpiece and the tool was characterized by friction coefficient, the value of which is shown in Table III.

TABLE IIIII
Adopted Values of Friction Coefficient

Machined material	**Rake angle γ,°**	**Friction coefficient for cutting speed v, m/min**			
		100	**175**	**250**	**300**
C45	+10	0.5	0.43	0.37	0.37
41Cr4	+10	0.55	0.47	0.44	0.42
	0	0.45	0.41	0.38	0.38
	-10	0.38	0.36	0.34	0.34
X10CrNiTi18–9	+10	0.47	0.42	0.38	0.38

When setting the temperature state, a value of room temperature was accepted as the initial condition in all calculated nodes, i.e. 20°C. Viewing its development, we proceeded from the fact that at the moment of stable flow chip formation, after the thermal balance has been reached, the stationary thermal field is formed in the cutting wedge of tool, because all three thermal sources do not change their positions. Mathematical description of temperature fields in solid bodies is given with the help of differential equation for thermal conductivity, depending on the body point temperature with coordinates, time and thermal conductivity coefficient. To solve the equation it is necessary to apply additional initial and boundary conditions to the function. The initial conditions fix the state of temperature field of bodies at zero time. The boundary conditions are conditions of surface interaction with environment and other bodies.

The calculation was done using the following parameters

- type of solver – iterative sparse; applying Incomplete Choleski's algorithm with preliminary data processing;
- making entries of the result in the object file with frequency 10 increments with a view to reducing its size;
- saving the intermediate results of the calculation in a separate file to allow the repeated start of calculation in case of its abrupt interruption.

When the cutter passes in the area of chip formation, we can see a regular picture of the constrained cutting with a typical start of ship curling (Fig. 4). Therefore, the effectiveness is confirmed of MSC.Marc software product application for modelling the cutting process, and correctness in the assumptions made, about what a conclusion was made in accordance with the results of the modelling of free cutting. It must be noted that in the area adjoining to the tool minor cutting edge the process of the residual ridge formation can be seen.

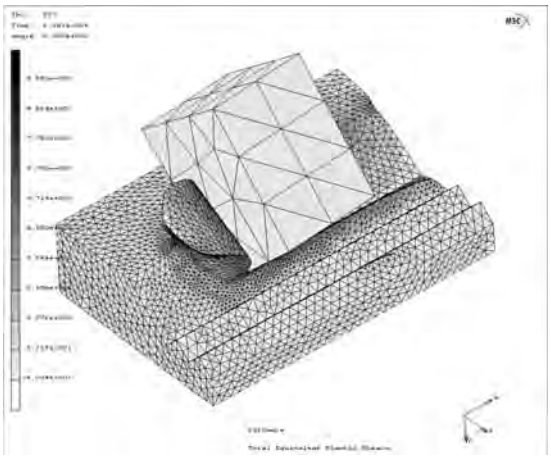

Fig. 4. Chip separation in the process of the constrained cutting with the start of its curling according the modelling results

To identify the regularities of residual ridge formation it was necessary to establish a value of plastic displacement of metal, strained when being cut, along the minor cutting edge.

In general view the strain-stressed state of the area we are interested in is shown in Fig. 5,a and 5,b (cutter is hidden). Values and distribution of equivalent stresses entirely correspond to the notions of the stressed state in a cutting area. Maximum stresses are concentrated on the conditional shear plane (890…1000 MPa), the lesser ones – on the surfaces formed (210…550 MPa), and also small stresses on the next residual ridge (100…210 MPa). It shows that during the cutting process the stresses spread relatively far beyond the chip formation area.

Shown in Fig. 5,b field of the total equivalent plastic strain shows that the strain is developed to the conditional shear plane (values vary within 0.7…1.4). Maximum strains are observed in the cutter face – chip contact area – 5.6…6.3. The situation is coincidental with Zorev's opinion ([19]) that the strain in the secondary strain area can be 20 times in excess of the strain found in the conditional shear plane. Large strain also takes place on the surfaces formed, and also at the top of the residual ridge (up to 4.2), because here is a boundary of separation of chip material from a workpiece.

The analysis included nodes of calculation, being arranged at the same level and distance 0.3 mm from the cutter face. They were arranged in such a way that the whole surface of the residual ridge could be covered (Fig. 6). The results of study of displacements along axis y for the nodes found at the top of the residual ridge, in the middle and in its hollow, are shown in calculated steps in Fig. 6. It shows that even in the hollow of residual ridge the plastic displacement of material is observed, although in far smaller sizes than at the top.

Fig. 7 shows variation of the metal displacement intensity during the residual ridge formation throughout its height. It is much greater in the area of ridge height than in the hollow. Moreover, the node displacements are not even, and have extremum at L=40%, i.e. at the moment of the cutter pass. Further occurs a backward movement, slightly decreasing the ridge height, i.e. material "is pulled back" from the residual ridge by the cutter being displaced. This process ends with the cutter passing an interval approximately equal to 90% from the overall length. There also occurs the formation of stable residual ridge. This implies that the accepted cutter displacement at the distance 0.7 mm was sufficient.

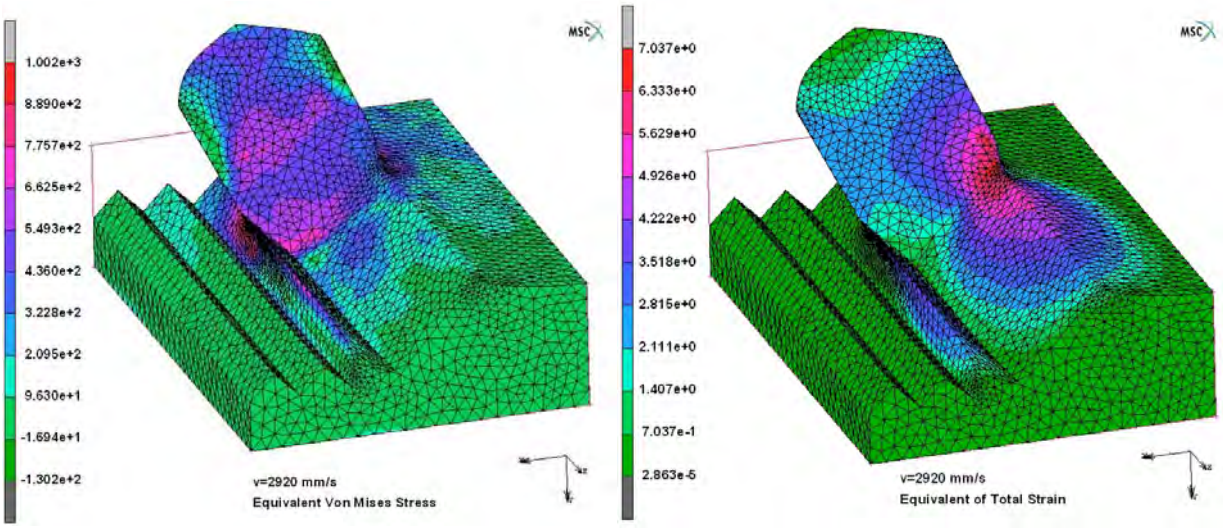

(a) (b)

Fig. 5. Mises stressed state (a) and strained state (b) in the process of the constrained cutting

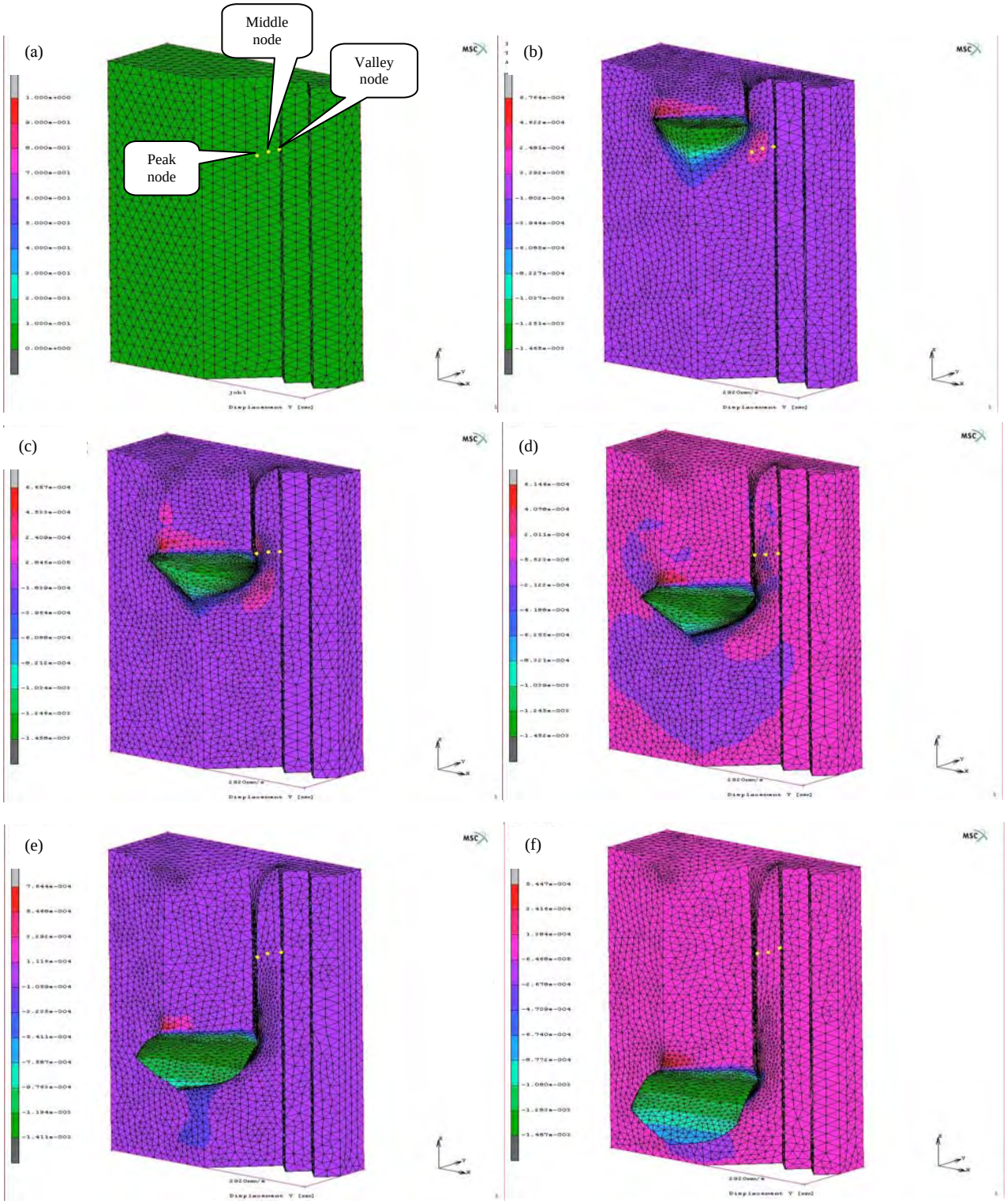

Fig. 6. Relative displacement of material along y-axis for initial status (a); 20% (b); 40% (c); 60% (d); 80% (e); 100% (f) from the set cutter displacement

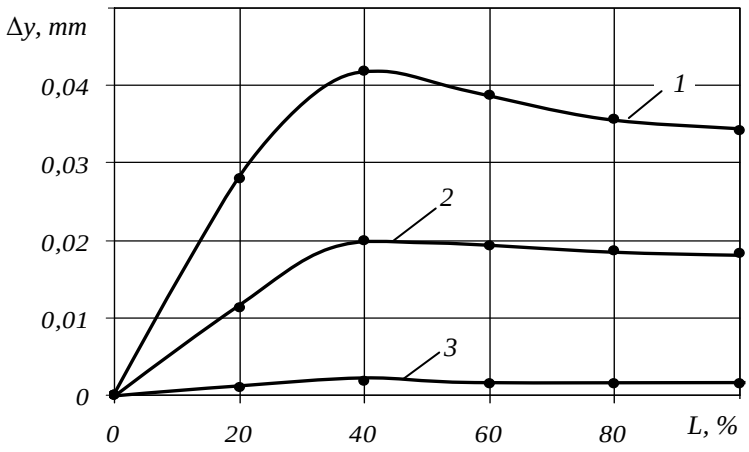

Fig. 7. Dependence of the displacement along y-axis y from the overall length (%), covered by the cutter, for top node (1), middle node (2) and valley node (3) of the residual ridge

A process of determining the height of irregularity strain component also required scrutinizing an adjacent hollow, having formed earlier, since there occurs plastic strain and metal displacement, spreading to the whole volume of irregularity formed. This is shown in Fig. 8, where a picture of plastic flow of metal in plan is presented. It is clearly seen that maximum displacements of the metal being cut are localised along the cutting edges. Accordingly, both sides of the residual ridge become strained. Metal displacement is also observed to the side of the surface being machined, which corresponds to linear turning realized in practice.

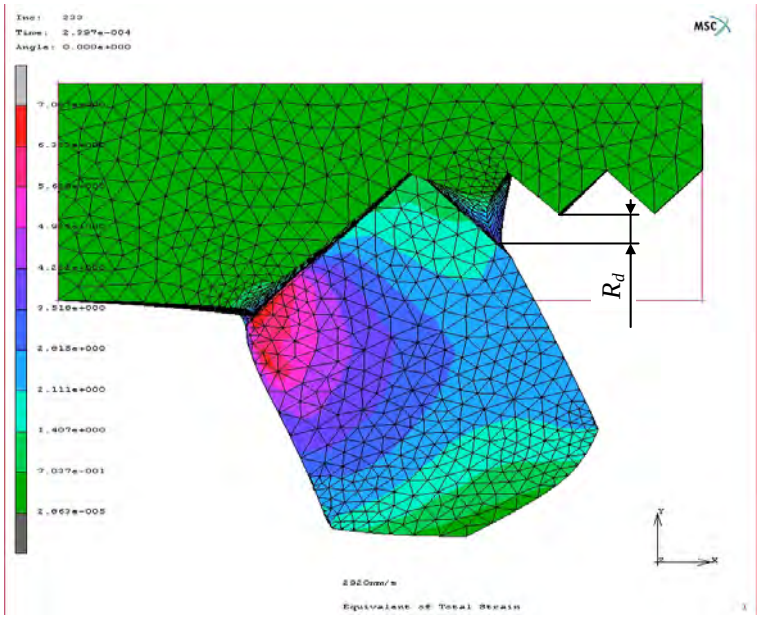

Fig. 8. Plan view of side plastic flow of material in the process of the residual ridge formation (cutter is hidden)

III. Surface Microprofile According to the Modelling Results

The microirregularity height strain component can be found as the difference of coordinates of the nodal points on the peak and in the valley of residual ridge and the known value of geometrical component. Based on the results of calculations of the finite element models, the initial parameters are shown in Table II, graphic dependences were obtained of the strain component of height parameter of roughness from displacement of type of the cutter shown in Fig. 7. As an example in Fig. 9,a a graph is given of the microirregularity height strain component dependence on the cutting route for some cutting speeds. Such dependence is typical of all cases studied. As the cutter is displaced, in the beginning rather intensive growth occurs of the microirregularity strain component with subsequent stabilization of its value which reflects the end of transients. The graph "cutting route" – microirregularity strain component" made it possible to obtain the dependence $R_d=f(v)$ clearly. That is what was being realized for the steady cutting process (Fig. 9,b).

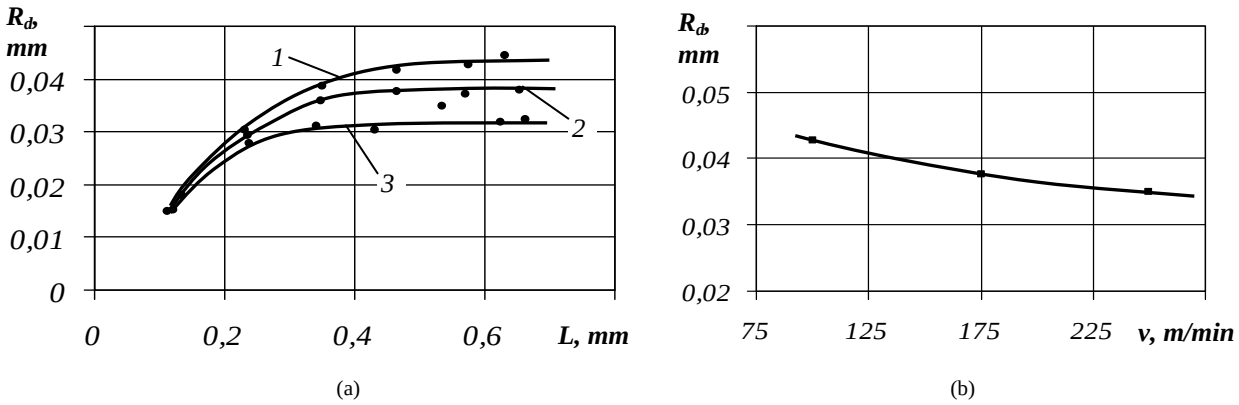

Fig. 9. Dependence of microirregularity strain component R_d on the cutter displacement L when machining 41Cr4 steel at cutting speed v: 1 – 100 m/min; 2 –175 m/min; 3 –250 m/min (a);
Dependence of microirregularity strain component R_d on the cutting speed v when machining 41Cr4 steel (b)

As a result of these constructions, dependences were established of the irregularity height strain component on an minor tool cutting edge angle, cutting edge inclination angle, rake angle, feed and cutting speed for steels 41Cr4, C45 и X10CrNiTi18–9. For a clearer pattern, without being strongly tied to the geometrical component R_g, the results are expressed by relation R_d / R_g. The corresponding graphs are shown in Fig. 10.

As is seen, a value of the strain component varies in a wide range, and may surpass the geometrical component. The common thing for them is the identical behaviour of the microirregularity component strain dependences on machining parameters for all materials investigated. Influence of mechanical features of steels on the height of residual ridge is small but unequivocal. The strain component is the least for X10CrNiTi18–9 steel and the largest for C45 steel. The component values in all cases are close to the values corresponding to X10CrNiTi18–9 steel. It can be explained by the fact that 45 steel has the least strengthening, in consequence of which the metal being cut becomes strained at a greater degree.

A reason for reducing the relation R_d / R_g with an increase in feed is obvious because, in doing so, the geometrical component increases in direct proportion. Along with it, the dependence $R_d / R_g = f(f)$ has a curvilinear shape, consequently, of change of the strain component. For the case with variable feed values the models were calculated, in which the tool displacement was 0.7 mm for feeds 0.05 and 0.1 mm/rev, 1.25 mm for feed 0.15 mm/rev and 1.8 mm for feed 0.2 mm/rev when the other parameters are unchangeable. This was done for the purpose that with the cutter's passing, the residual ridge would be fully formed. As a result, it was established that with an increase in feed there is some increase in the value of strain component of the residual ridge height.

With an increase in cutting speed the value of strain component slightly decreases, in the range of 10…15%. This agrees with the slight decrease in chip compression in the area of high cutting speeds.

The influence of rake on the relation R_d / R_g is worth noting (Fig. 10,c). When it increases, despite a decrease in degree of the strain of metal being cut, which is expressed by chip contraction, the microirregularity strain component increases. Explanation for the increase in the microirregularity strain component with the increase in rake, even with the decrease in the degree of strain, was given by Isaev ([5]). The reason is that, in doing so, the rake decreases on the minor cutting edge. Consequently, the degree of strain of the metal being cut increases in the area adjacent to the minor cutting edge, and this is expressed in a decrease in the angle of displacement in this area ([6], [19]). Agreement is also can be noted in alteration in the height of microirregularity strain component with alteration in the direction of chip flow. As follows from Fig. 11 and 12,a, with the increase in rake, the chip flow angle decreases, i.e. the direction of its motion approaches the direction of the free side of the residual ridge. As a consequence, duration grows of the contact of moving chip with the residual ridge being formed.

Influence of the cutting edge inclination angle on the strain component of microprofile is shown in Fig. 10,d. Its growth with an increase in the angle λ is to be also connected with the change of chip flow direction to the side of machined surface (Fig. 12,b).

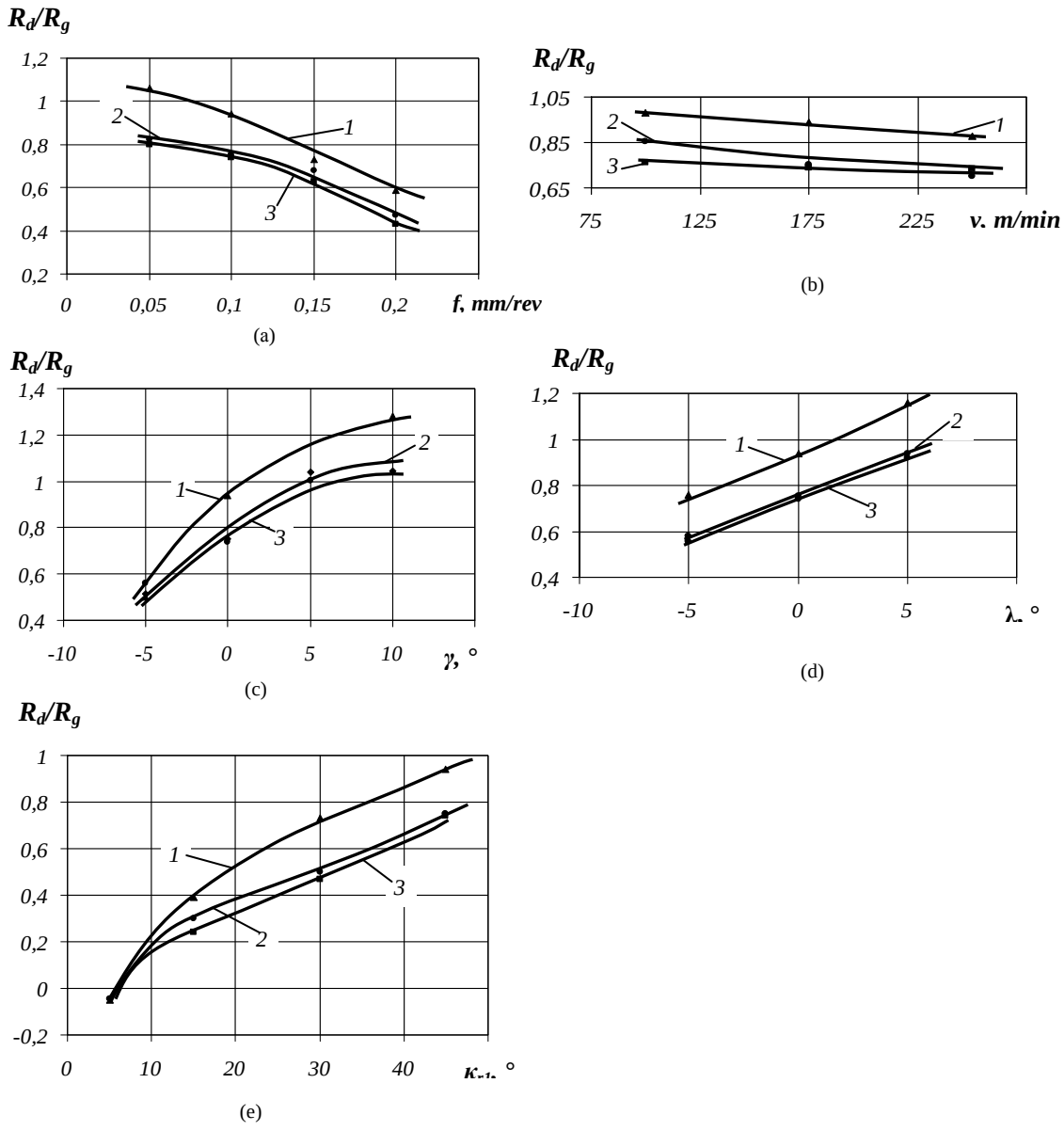

Fig. 10. Dependence of relation of the strain component to the geometrical component R_d / R_g on: feed f(a), cutting speeds v(b), rake angle γ (c), cutting edge inclination angle λ (d), minor cutting edge angle κ_{r1} (e) for steels: C45 (1), 41Cr4 (2) and X10CrNiTi18–9 (3)

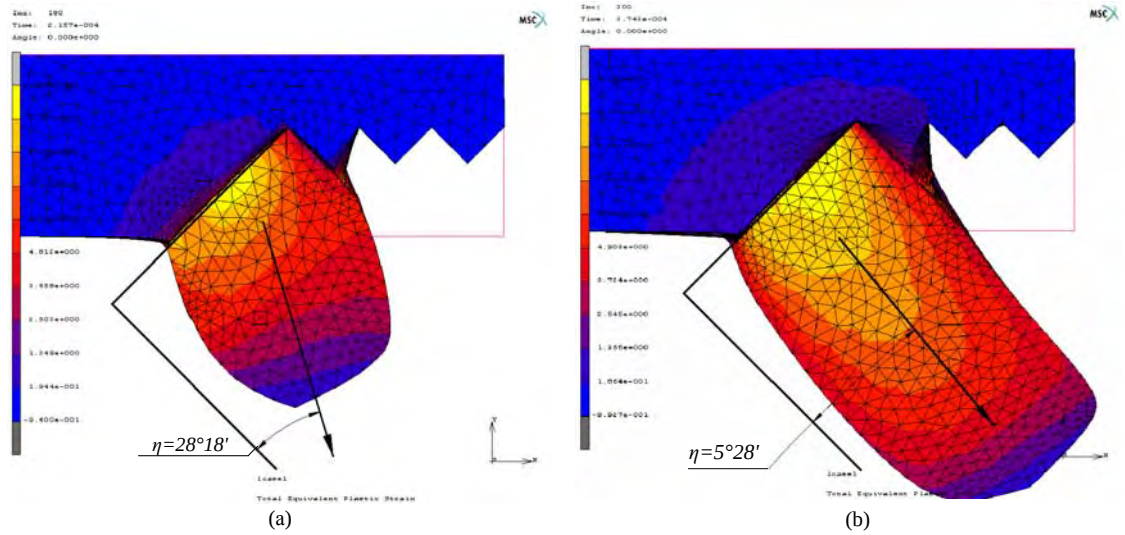

Fig. 11. Chip-flow angle η when cutting 41Cr4 by cutter with rake angle γ= -5° (a) and γ= +5° (b)

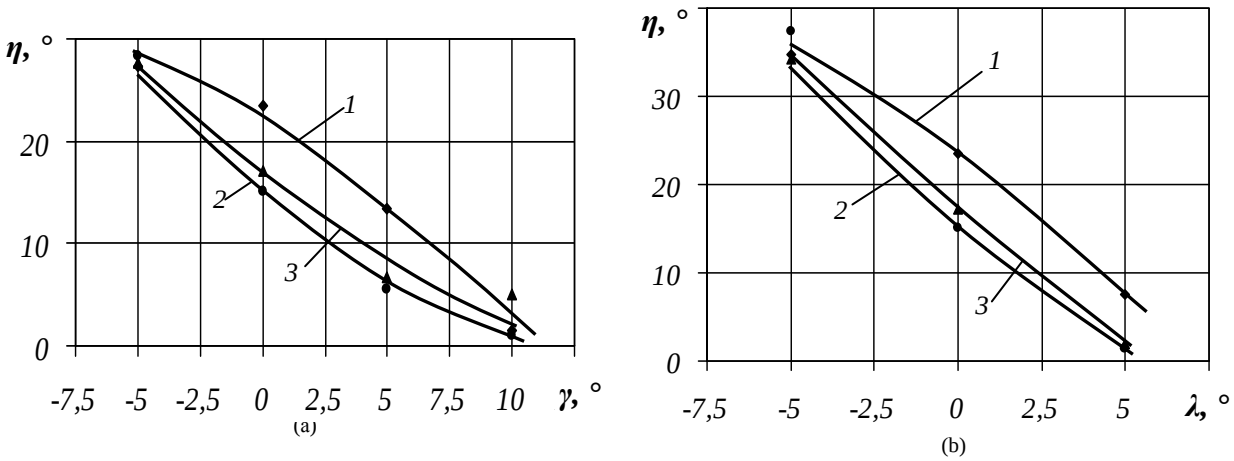

Fig. 12. Chip-flow angle with respect to tool rake angle γ (a) and cutting edge inclination angle λ (b) for steels: C45 (1), 41Cr4 (2) and X10CrNiTi18–9 (3)

Dependences $R_d = f(\kappa_r)$ and $R_d = f(\kappa_{r1})$ can be viewed together, since alteration of angles in plan is equally reflected on the cross section of cut. A series of models here was calculated only for the minor cutting edge angle.

An increase in these angles, as it results from ([6], [7]), is accompanied by approximation of the form of cross section of the metal being cut to the triangular one when its strain near the minor cutting edge is more significant. As a result of such displacement it is necessary to view the growth of microirregularity strain component when the major and minor cutting edge angles increase. In connection with the views set forth, it is possible to obtain even a negative value of the strain component when a value of the minor cutting edge angle is close to zero. In this regard, chip flow is directed from the minor cutting edge, and this will reorient the flow of material, forming the residual ridge, to the opposite one.

Summing up the performed analysis of the influence of process parameters on the microprofile strain component, it can be stated that the results of modelling agree with the experimental data, and blend in with the general idea of regularities of the milling process.

IV. Comparing the Results of Modelling with the Experimental Data

Adequacy of the surface roughness dependences obtained in the modelling process on the machining parameters was examined by comparing them with the experimental data for turning X10CrNiTi18–9 steel.

According to the modelling results, power law dependence was calculated $R_d / R_g = f(f, v, \gamma, \lambda, \kappa_{r1})$ using the least-square method

$$\frac{R_d}{R_g} = 1.91e5 \cdot f^{-0.424} \cdot v^{-0.121} \cdot (20+\gamma)^{1.19} \cdot (20+\lambda)^{0.915} \cdot \kappa_{r1}^{1.017}.$$

Using formula and the initial data for experiment (geometry of the tool and machining conditions), curves 1, 2, 3 were built (Fig. 13). For experimental curves 4, 5, 6 Fig. 13 an assumption was made that R_d =Rz- R_g , i.e. the strain component of the height parameter of roughness also includes all other components minimized during the experiment. Consequently, the certain divergence of data is natural, and is 20…30%.

The most discrepancy of experimental and model data (curves 1 and 4) is observed at less feeds (f=0.11 mm/rev), which says about complicated processes occurring in the cutter-chip area, when a value of tool edge radius exerts much influence on the residual ridge being formed. According to Zorev ([19]), this influence occurs in a case when relation of the cut layer thickness to the rounded cutting edge radius is less than 10.

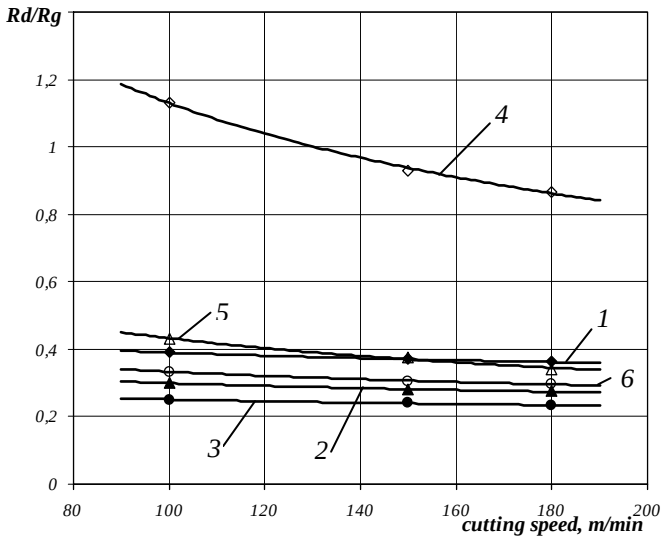

Fig. 13. Influence of cutting speed on R_d / R_g relation, when cutting X10CrNiTi18–9 steel, as per results of FE modelling (1 – *f*=0.11 mm/rev; 2 – *f*=0.21 mm/rev; 3 – *f*=0.31 mm/rev), as per the experimental data (4 – *f*=0.11 mm/ rev; 5 – *f*=0.21 mm/rev; 6 – *f*=0.31 mm/rev)

V. CONCLUSION

In general, the developed model of constrained cutting and the dependences obtained with certain assumptions rather truly describe processes occurring in the chip flow area, and can be used for further studies.

ACKNOWLEDGMENT

The work described in the given paper is carried out by financial support of Russian Government within the framework of the integrated project "Automation and efficiency increase of production processes and preproduction of aircraft items of new generation at IRKUT Corporation by scientific support of Irkutsk State Technical University".

REFERENCES

[1] S. Belhadi, T. Marouki, J.-F. Rigal and L. Bouanouar, “Experimental and Numerical Study of Chip Formation During Straight Turning of Hardened AISI 4340 Steel”, *J. Engineering Manufacture*, vol. 219, pp.515-524, 2005.
[2] F. Chinesta, L. Filice, F. Micari, S. Rizzuti and D. Umbrello, “Assessment of material models through simple machining tests”, *International Journal of Material Forming*, vol. 1, Supplement 1, pp.507-510, 2008.
[3] M.G. Goldschmidt, G.D. Del and G.L. Kufarev, “Stress condition during segmented chip formation”, *Izvestiya TPI*, vol. 139, pp.238-244, 1966. (in Russian)
[4] M.L. Heifetz and C.V. Sychev, “Modeling by method for cutting process finite elements with wear resistant tool”, *Journal of computer in information technologies*, No. 5, pp. 11-17, 2007 (in Russian)
[5] A.I. Isaev, *Process of formation of surface layer in metal machining*, Moscow: MachGIZ, 1950. (in Russian)
[6] G.L. Kufarev, K.B. Okenov and V.A. Govoruhin *Chip forming and condition of machined surface during conventional cutting*, Frunze: Mektep, 1970. (in Russian)
[7] T.N. Loladze, *Chip forming in metal cutting*, Moscow: MachGIZ, 1952. (in Russian)
[8] T.T. Öpöz and X. Chen, “Finite element simulation of chip formation”, *School of Computing and Engineering Researcher’s Conference, University of Huddersfield*, pp.166-171, 2010.
[9] T. Özel and E. Zeren, “Numerical modelling of meso-scale finish machining with finite edge radius tools”, *Int. J. Machining and Machinability of Materials*, vol. 2, No. 3, pp.451–468, 2007.
[10] O. Pantale, J.-L. Bacaria, O. Dalverny, R. Rakotomalala and S. Caperaa, “2D and 3D Numerical Models of Metal Cutting with Damage Effects”, *Comput. Methods Appl. Mech. Engrg.*, vol.193, pp.4383-4399, 2004.
[11] V.N. Poduraev, *Cutting difficult-to-machine materials*, Moscow: Vischaya Shcola, 1974. (in Russian)
[12] M.F. Poletika, *Contact loads on the tool cutting surfaces*, Moscow: Machinostroenie, 1969. (in Russian)
[13] A. Raczy, W.J. Altenhof and A.T. Alpas, “An eulerian finite element model of the metal cutting process”, *8th International LS–DYNA User Conference. Session 9 Metal Forming*, pp. 11–25, 2004.
[14] A.M. Rosenberg and A.N. Eremin, *Elements of theory of metal cutting process*, Moscow: MachGIZ, 1956. (in Russian)
[15] A.M. Rosenberg, O.A. Rosenberg, E.I. Gricenko and E.K. Posviatenko, *Quality of surface machined by means of straining draw*, Kiev: Naukova Dumka, 1977. (in Russian)
[16] N. Ruttimann, S. Buhl and K. Wegener, “Simulation of single grain cutting using SPH method”, *Journal of Machine Engineering*, vol. 10, No. 3, pp. 17-29, 2010.
[17] Ship-Peng Lo “An analysis of cutting under different rake angles using the finite element method”, *Journal of Materials Processing Technology*, pp. 143-151, 1999.
[18] V.A. Zaloga, “Studying the cutting force alteration dynamics in the cutting-in process by the method for finite elements”, *Vestnik SumDU. Technical sciences series*, No. 3, pp. 13-24, 2008 (in Russian)
[19] N.N. Zorev, *Issues of mechanics of metal cutting process*, Moscow: MachGIZ, 1956. (in Russian)